PCCP

Accepted Manuscript

ROYAL SOCIETY OF CHEMISTRY

www.rsc.org/pccp

Journal Name

RSCPublishing

ARTICLE

Sol-gel Transition Accelerated by Co-assembly of Two Components in Supramolecular Hydrogels

Cite this: DOI: 10.1039/xoxxoooooox

Keigo Matsumoto,[a,b,*] Atsuomi Shundo,[a,c,d,*] Masashi Ohno,[b] Kowichiro Saruhashi,[b] Nobuhide Miyachi,[b] Nobutomo Tsuruzoe[b] and Keiji Tanaka[a,c,d,*]

Received ooth January 2012,
Accepted ooth January 2012

DOI: 10.1039/xoxxoooooox

www.rsc.org/

N-palmitoyl-Gly-His (PalGH) and glycerol monopalmitate (GMP) in water co-assembled into fibrils with twisted ribbon structures and formed a homogeneous network, resulting in gel formation. Shaking the gel easily broke the fibril network leading to a sol in which high and low fibril density regions exist. After a period at room temperature, the higher density regions became interconnected. The spontaneous sol-gel transition did not take place for a gel made from only PalGH. Also, during the transition, the aggregation state of the co-assembly remained unchanged at a molecular level, unlike the fibril network. Thus, it can be claimed that the sol-gel transition is not associated with the assembled molecular configuration, but with the change in the fibril network. This knowledge might be useful for understanding and controlling sol-gel transition, thereby leading to the design and functionalization of hydrogels.

1. Introduction

Amphiphilic molecules dispersed in water often self-assemble with a large aspect ratio, leading to the formation of a three-dimensional network. The network may produce a physical hydrogel, a so-called supramolecular hydrogel (SMG). Unlike conventional polymeric hydrogels, SMGs undergo a phase transition between the sol and gel states, in response to external stimuli such as temperature,[1] pH,[2] ions[3] and light.[4] Of these stimuli, sol-gel transition induced by mechanical stress (or strain) has received increasing attention.[5] A SMG easily becomes a fluid, namely a sol, by mechanical disruption. Over time and without any heating, however, the sol sometimes spontaneously returns to the gel state. Such a feature of SMGs makes them promising candidates in a variety of applications, such as injectable gels,[6] carriers for drug delivery,[7] cell scaffolds,[8] sprayable materials,[9] self-healing materials[10] and separation medium.[11]

A common strategy to obtain SMGs that exhibit the sol-gel transition is the chemical modification of molecules. So far, great efforts have been made to study the relationship between the chemical structure of molecules and the sol-gel transition behavior.[5b,5g,12] Such an approach has provided a better understanding of how to confer the sol-gel transition onto SMGs. For the moment, however, it is not easy to obtain desirable SMGs and the method remains unclear. Thus, to design and control the sol-gel transition of SMGs, an alternative methodology is required.

Recently, SMGs composed of two kinds of molecules, namely two-component gels, have been studied to control the physical properties of SMGs.[13,14] In the two-component gels, two molecules co-assemble into a fibrous network structure. This means that the physical properties of two-component gels could be easily tuned by varying the composition ratio of the two components. We have previously demonstrated regulation of the viscoelastic properties of a SMG composed of *N*-Palmitoyl-Gly-His (PalGH) and sodium palmitate (PalNa).[14] The PalGH molecules in water form lamellar-like assemblies, which stack into sheet-shaped aggregates, resulting in the evolution of a three-dimensional network structure. Once PalNa is added to PalGH, alkyl groups of PalNa are incorporated into the hydrophobic cores of the lamellar assembly of PalGH, leading to the change in the hierarchical structure, thereby altering the bulk viscoelastic properties of the hydrogel. In this study, we focus on an SMG composed of PalGH and glycerol-1-monopalmitate (GMP), which is chosen as a modulator for the lamellar assembly of PalGH. The incorporation of the palmitoyl group of GMP into the PalGH assemblies can be expected. Also, the glycerol residue in GMP has a potential to form hydrogen bonds with the amide moiety of PalGH. These structural features may regulate the sol-gel transition of the SMG.

2. Experimental

2.1 Materials

PalGH was synthesized following the method previously reported.[15] GMP purchased from Tokyo Chemical Industry Co. Ltd. was used as received. Scheme 1 shows the chemical structure of PalGH and GMP. Water was deionized with Elix UV3 (Millipore Co.), and was used for the hydrogel formation. Deuterated water (D_2O) was purchased from SIGMA-Aldrich Co. LLC., and was used for Fourier-transform infrared (FT-IR) spectroscopy. For confocal laser scanning microscopy (CLSM), 9-(diethylamino)-5H-benzo[*a*]phenoxazin-5-one (Nile Red) was purchased from Tokyo Chemical Industry Co. Ltd., and was used as received.

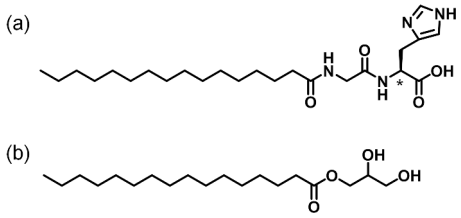

Scheme 1 Chemical structures of (a) *N*-palmitoyl-Gly-His (PalGH) and (b) glycerol-1-monopalmitate (GMP).

2.2 Gel preparation

PalGH and/or GMP were well dispersed into 4 mL of pure water and the mixture was heated at 373 K for 1 h in a dry bath incubator (AS ONE Co. Ltd.). To suppress water evaporation, sealed vials (AS ONE Co. Ltd.) were used. The resulting hot dispersion was left undisturbed for 24 h at room temperature. Keeping the total concentration at 20 mM, the molar percentage of GMP against PalGH (*X*) was varied - 0, 30, 50, 70 and 100 %. Rheological measurements were made using an MCR 310 rheometer (Anton Paar Japan K. K.) In all measurements, a cone-type plate with a diameter of 50 mm and a tilt angle of 1.0° was used.

The gels with $X = 0$, 50 and 100 % were shaken by a vortex mixer (M&S instruments Inc.) for 30 s. The resultant sols were left undisturbed for 24 h at room temperature to observe the sol-to-gel transition.

2.3 Differential scanning calorimetry

Differential scanning calorimetry (DSC) measurements were carried out using a DSC 7020 (Hitachi High-Tech Science Co.). An aqueous dispersion of PalGH and/or GMP obtained by heating at 373 K was placed in a sliver pan and then sealed. The sample was left undisturbed for 24 h to reach equilibrium prior to measurement. In all measurements, a water-containing pan was used as a reference. The specimen was heated up to 353 K at a rate of 5 K min^{-1} under a dry nitrogen purge and then cooled down to 293 K at a rate of 10 K min^{-1}. This cycle was repeated three times. The third scan was used to judge thermal dissociation of the molecular assembly.

2.4 Fourier-transform infrared spectroscopy

For the FT-IR measurements, PalGH and/or GMP were/was dispersed in D_2O by heating at 373 K. The resulting solution was left undisturbed for 24 h at room temperature. The resultant sample was sandwiched between CaF_2 windows with a 0.2 mm-gap. The FT-IR spectra were recorded using a FT/IR-620 spectrometer (JASCO Co.) equipped with a triglycine sulfate (TGS) detector. All spectra were obtained with a resolution of 4 cm^{-1} and 64 scans at room temperature.

2.5 Small-angle X-ray scatting measurements

Small-angle X-ray scatting (SAXS) experiments were carried out at the BL40B2 beamline of SPring8 (Japan). The wavelength of incident X-rays and the sample-to-detector distance were 0.10 nm and 2179 mm, respectively. Scattered X-rays were recorded using a Rigaku R-AXIS IV+++ system (300 × 300 mm imaging plate). Exposure time was 300 s. By circular averaging the two-dimensional pattern on the imaging plate, a one-dimensional scattering profile of the sample was obtained.

2.6 Transmission electron microscopy

A piece of the sample was placed on a copper grid (Okenshoji Co. Ltd) and then dried under ambient atmosphere. Transmission electron microscopic (TEM) images were acquired with a HT7700 scanning transmission electron microscope (Hitachi High-technologies Co. Ltd.). The observations were made at an accelerating voltage of 100 kV.

2.7 Confocal laser scanning microscopy

An aqueous dispersion of PalGH and/or GMP containing 60 μM of Nile Red pre-warmed at 373 K was placed in a glass bottom dish (Matsunami Glass Inc. Ltd.) and sealed with a glass cover using vacuum grease. The sample was left undisturbed for 24 h prior to observation with a confocal laser scanning microscope equipped with a semiconductor laser and a DAPI filter block (LSM700, Carl Zeiss Microscopy Co., Ltd.).

3. Results and discussion

3.1 Co-assembly of two molecules

PalGH is an amphiphilic molecule having a palmitoyl group and peptide residues, as shown in Scheme 1. It should be noted that the histidine residue in PalGH is chiral (*S*-configuration). GMP, which possesses a palmitoyl group and glycerol residue, is a racemic mixture of GMPs having glycerol residues with an equal proportion of *R*- and *S*-configurations. First of all, we examined the co-assembling behavior of PalGH and GMP in water as a function of their compositions. Fig. 1 shows photographs of the PalGH-GMP-water mixtures with various molar percentages of GMP against PalGH (*X*) - 0, 30, 50, 70

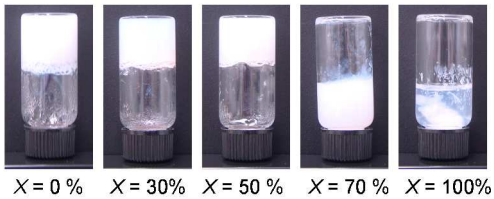

Fig. 1 Photographic images of the PalGH-GMP-water mixtures with $X = 0$, 30, 50, 70 and 100 %.

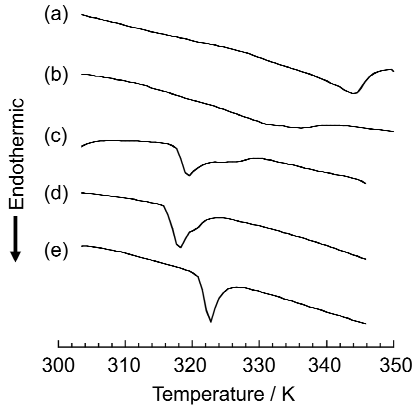

Fig. 2 DSC thermograms of the PalGH-GMP-water mixtures with (a) $X = 0$, (b) 30, (c) 50, (d) 70 and (e) 100 %. Each curve is vertically shifted for clarity.

and 100 %. When PalGH was dissolved in water by heating at 373 K and then subsequently cooled slowly to room temperature, it formed a hydrogel. In the case of mixtures with X = 50 % or less, hydrogels were obtained but no hydrogels were obtained from mixtures with $X > 50$ %.[16]

Fig. 2 shows DSC thermograms of the PalGH-GMP-water mixtures with $X = 0$, 30, 50, 70, and 100 %. The homo PalGH gel ($X = 0$ %) provided an endothermic peak at 343 K as a peak top temperature in the heating process. This peak can be assigned to the thermal dissociation of the assembly of the PalGH molecules, which is accompanied by thermal gel-to-sol transition.[17] The peak shifted to a lower temperature as X was increased up to 70%. However, the peak top temperature for the homo GMP sol (X = 100 %) was higher than the peak top temperatures for $X = 50$ and 70 %. These results imply that the GMP molecules incorporate into the assembly of PalGH.

Fig. 3 shows the FT-IR spectra of the PalGH-GMP-water mixtures with X = 0, 30, 50, 70, and 100 %. Deuterated solvents were used for the preparation of all samples and the contribution from the solvent was removed by subtracting the solvent spectrum corrected using a scaling factor. For the homo PalGH hydrogel ($X = 0$ %), absorption peaks assignable to the symmetric and antisymmetric C-H stretching vibrations of methylene groups (ν_{s,CH_2} and ν_{as,CH_2}) appeared at 2849 cm^{-1} and 2919 cm^{-1}, respectively. Also, absorption peaks assignable to the C=O stretching vibration in the amide moiety ($\nu_{C=O}$) appeared at 1644 cm^{-1} and 1607 cm^{-1}. Another peak at 1658 cm^{-1} due to the C=O moiety in carboxyl groups (ν_{COOH}) was also observed. We have previously found that in the case of the homo PalGH gel: (1) the alkyl chain in PalGH is extended with a higher population in the *trans* conformation and (2) the amide moieties form weak and strong hydrogen bonds, as evidenced by the fact that the wavenumbers for the $\nu_{s,CH2}$, $\nu_{as,CH2}$ and two $\nu_{C=O}$ peaks are lower than those for PalGH homogeneously dissolved in dimethyl sulfoxide (DMSO).[14]

In the case of the PalGH-GMP-water mixtures, the peak positions of ν_{s,CH_2} and ν_{as,CH_2} were independent of the X value. However, this was not the case for the peaks located in the range of 1800-1500 cm^{-1}. The $\nu_{C=O}$ peaks of PalGH shifted to a higher wavenumber with increasing X up to 70 % (1645 and 1608 cm^{-1} for $X = 30$ %; 1650 and 1634 cm^{-1} for X =50 %; 1654 and 1635 cm^{-1} for $X = 70$ %). This indicates that the hydrogen bonds among the amide moieties became weaker upon the addition of GMP. In the mixtures with X = 30, 50 and 70 %, two peaks due to the C=O moiety in the ester group (ν_{COO}) of GMP were also observed at 1733 cm^{-1} and 1703 cm^{-1}. The wavenumbers of the two peaks were lower than that of the ν_{COO} peak observed for X = 100 % (1736 cm^{-1}). Thus, the two ν_{COO} peaks can be assignable to the ester groups that form weak and strong hydrogen bonds. These results imply that the palmitoyl groups of GMP incorporate into the hydrophobic core of the PalGH assembly. As a result of the incorporation, the ester groups in GMP become closer to the peptide residues in PalGH. This activity might induce the dissociation of some of the hydrogen bonds of the amide moieties of PalGH, and result in the concurrent formation of hydrogen bonds between the amide moiety of PalGH and the ester group of GMP.

Fig. 4 shows the SAXS profiles for the PalGH-GMP-water mixtures with $X = 0$, 30, 50, 70, and 100 %. The homo PalGH gel ($X = 0$ %) showed sharp peaks at the scattering vectors (q) of 1.3 and 2.6 nm^{-1}, corresponding to domain spacings (d) of 4.9 and 2.5 nm, respectively. These are the first and second order peaks scattered from a lamellar assembly with an interlayer distance of 4.9 nm.[14] In the case of the mixtures with $X = 30$, 50 and 70 %, the sharp peaks were replaced by a broad

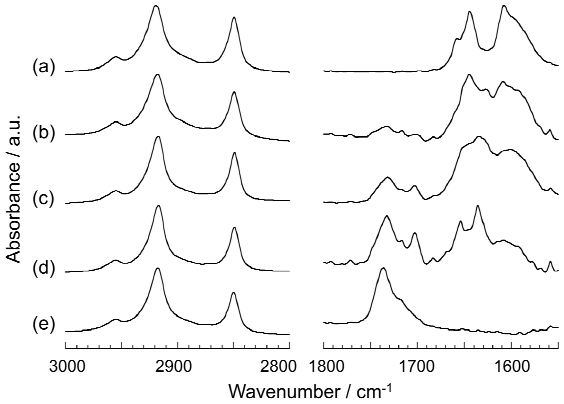

Fig. 3 FT-IR spectra of the PalGH-GMP-water mixtures with (a) $X = 0$, (b) 30, (c) 50, (d) 70 and (e) 100 %. Each spectrum is normalized and vertically shifted for clarity.

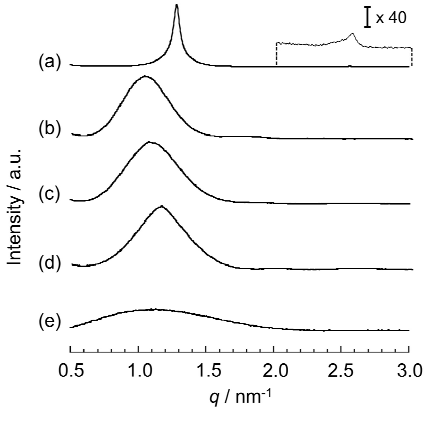

Fig. 4 SAXS profiles of the PalGH-GMP-water mixtures with (a) $X = 0$, (b) 30, (c) 50, (d) 70 and (e) 100 %. Each curve is normalized and vertically shifted for clarity.

peak. The peak was observed at q = 1.0 nm^{-1} (d = 6.1 nm) for X = 30 %, q = 1.0 nm^{-1} (d = 6.1 nm) for X = 50 % and q = 1.2 nm^{-1} (d = 5.4 nm) for X = 70 %. Such a broad scattering profile is often observed for micelle-like assemblies with a large aspect ratio.[18] Given that a fibrous micelle-like co-assembly is formed in the PalGH-GMP-water mixtures, it is most likely that the palmitoyl groups of GMP are incorporated into the lamellar-like assembly of PalGH.

3.2 Sol-gel transition

We examined the change in the fluidity of the homo and mixed gels during the process of shaking and aging. Fig. 5 shows photographs showing the variation in the physical state of the gels with X = 0 and 50 %. When the homo PalGH gel (X = 0 %) was broken up by shaking with a vortex mixer, it transformed into a sol state. After aging the sol for 24 h at room temperature, the sol state remained unchanged. However, this was not the case for the mixed gel (X = 50 %). Shaking the mixed gel also produced a sol but it returned to the gel state after aging for 24 h. This indicates that the incorporation of the GMP molecules into the PalGH assembly promotes the sol-to-gel transition.

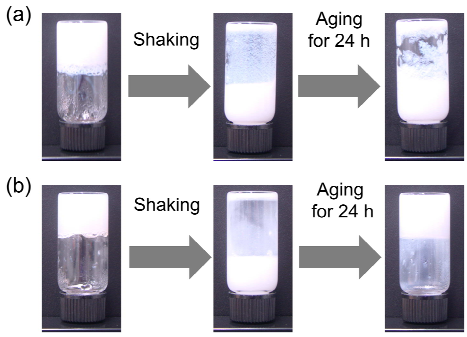

Fig. 5 Photographic images showing the variation in the physical state for (a) the homo gel (X = 0 %) and (b) the mixed gel (X = 50 %) during the shaking and aging process.

To address the mechanism of sol-to-gel transition in the mixed gel, the change in the molecular assembled states was examined by FT-IR and SAXS measurements. Fig. 6 shows the FT-IR spectra for the homo and the mixed gels (X = 0 and 50 %) during the shaking-aging process. In both mixed gels, the position of the absorption peaks was not changed during the process. This makes it clear that the states of the PalGH assembly and the PalGH-GMP co-assembly were preserved during the shaking-aging process. This was also supported by the SAXS measurements. There is no substantial difference in the SAXS pattern during the shaking-aging process, as shown in Fig. 7. These facts motivated us to examine structure at a relatively large scale; that is, we examined fibrous aggregates and their network.

3.3 Morphology of aggregates and network

To confirm morphological changes to the aggregates during the sol-gel transition, TEM observations were made. Fig. 8 shows the TEM images obtained for the homo and mixed gels (X = 0

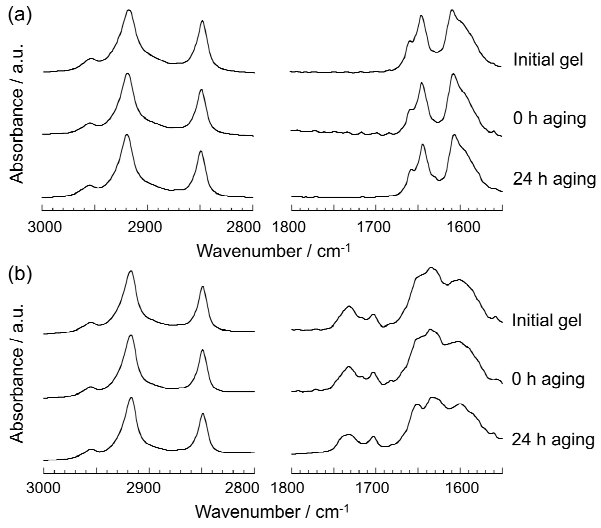

Fig. 6 FT-IR spectra for (a) the homo gel (X = 0 %) and (b) the mixed gel (X = 50 %) during the shaking and aging process. Each spectrum is normalized and vertically shifted for clarity.

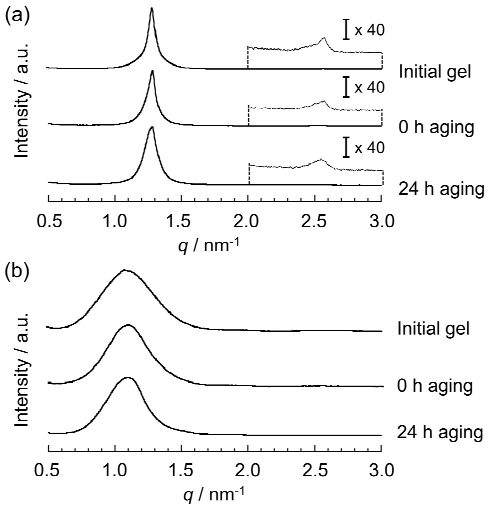

Fig. 7 SAXS profiles for (a) the homo gel (X = 0 %) and (b) the mixed gel (X = 50 %) during the shaking and aging process. Each curve is normalized and vertically shifted for clarity.

and 50 %) during the shaking-aging process. In the homo PalGH gel (X = 0 %), sheet-shaped aggregates were observed. The formation of the sheet-shaped aggregates can be reasonably understood if we assume that the lamellar assemblies stacked on top of each other.[14,19] In the case of the mixed gel, twisted ribbon-like aggregates with a relatively small width were observed. All of the ribbon structures were observed to twist to the right. Taking into account that the histidine residue in PalGH is chiral (*S*-configuration), the twisted structure could be induced from the histidine residue, like other chiral amphiphiles.[20] It should be noted that the formation of such a twisted structure was not observed for the aggregates composed of only PalGH. This might be due to the effect of curvature instability of the PalGH aggregates at a large width, which suppresses the formation of the twisted ribbon.[21]

Upon shaking and aging, the shape and size of the sheet-shaped aggregates in the homo PalGH gel were not changed.

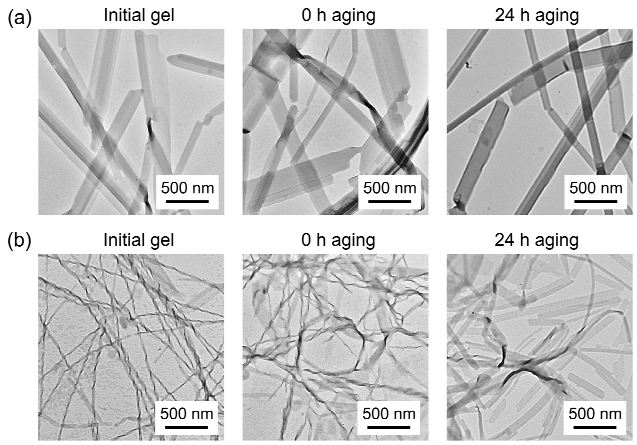

Fig. 8 TEM images for (a) the homo gel (X = 0 %) and (b) the mixed gel (X = 50 %) during the shaking and aging process.

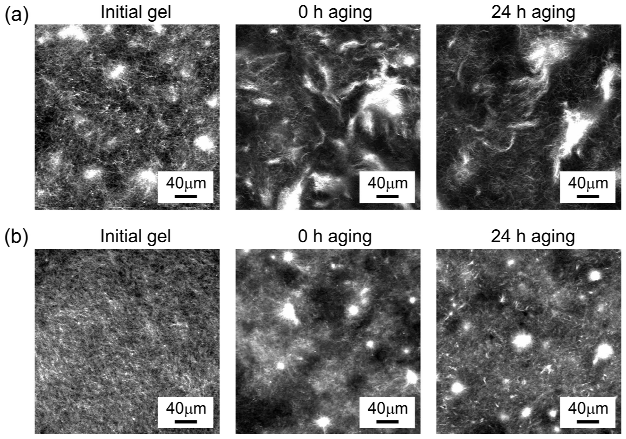

Fig. 9 CLSM images for (a) the homo gel (X = 0 %) and (b) the mixed gel (X = 50 %) during the shaking and aging process. The concentration of Nile Red was 60 μM.

On the other hand, the morphology of the twisted-ribbon like aggregates in the mixed gel changed after the shaking and aging process. When the mixed gel was shaken, both the twisted ribbons and the sheets were observed. After aging for 24 h, all of the twisted ribbons turned to sheets. Thus, it is obvious that the shaking and aging process induces the morphological change from twisted ribbons to sheets, although the reason for the change is not clear at the moment.

The network structure of the aggregates was also observed by CLSM. As a fluorescence probe, Nile Red was used. This dye has little solubility in pure water and localizes in the hydrophobic core of molecular assemblies.[22] This feature makes it possible to stain the assembly and to create contrast in the fluorescence microscopic image.[23] Fig. 9 shows the CLSM images obtained for the homo gel and the mixed gel (X = 0 and 50 %) during the shaking-aging process. In the homo PalGH gel (X = 0 %), fibrils and their network were observed. Although the network does not appear to be homogeneous, it covered the entire area observed. The fibrils and the network were also observed in the mixed gel (X = 50 %). In this case, the fibrils were denser and the resultant network was more homogeneous in comparison with the homo PalGH gel. Given that the aggregates in the mixed gel are smaller than those in the homo gel, as observed by TEM, the dense and homogenous network in the mixed gel makes sense.

In the sol obtained by shaking the homo PalGH gel, high and low density regions of the fibrils were observed, as evidenced by the presence of dark and light regions. These two regions remained even after aging for 24 h. On the other hand, the behavior of the fibrils in the mixed gel was different from that of the fibrils in the homo gel. High and low density regions were also generated in the mixed system after shaking. However, the areal size of the denser region was significantly larger than in the homo system. In addition, circular-shaped domains in which fibrils are thought to be extremely concentrated appeared in the denser regions. After aging for 24 h, the denser regions merged together leading to an expansion of the network over the area observed, although the shape and size of the circular domains did not change. Taking into account that network evolution is a necessary condition for gel formation,[24] it is quite reasonable that the system does not flow after aging for 24 h, as shown in Fig. 5(b). It is noteworthy that although the microscopic sol-gel transition occurs in the mixed state, no change was evident in the co-assembled state of PalGH and GMP. Thus, it can be claimed that the sol-gel transition reflects the change in the network structure of the fibrils.

Finally, we discuss the difference in the response behaviors between the homo and the mixed gels. The sol obtained by shaking changed back to a gel for the mixed gel but not for the homo gel. As mentioned above, right after shaking, the denser regions of the fibril network were much more expansive in the mixed system than in the homo system. This means that the denser regions were closer together in the mixed system. Taking into account that the sol-to-gel transition is based on network formation as a result of the interconnection of denser regions, it is reasonable that the aging time required to form the network, thereby inducing sol-to-gel transition, was shorter for the mixed system. Of course, such an explanation does not completely explain sol-gel transition where individual fibrils are dissociated and associated in complex ways. A more conclusive study on fibril diffusion including the phantom effect[25] will be reported in the near future.

4. Conclusions

We demonstrated the sol-gel transition of supramolecular hydrogels composed of PalGH and GMP. Once PalGH and GMP were mixed in water, the alkyl groups of GMP incorporated into hydrophobic cores of the lamellar-like assemblies of PalGH. Such an incorporation induces the molecular assembly to form fibrous micelle-like structures. Consequently, sheet-shaped aggregates, which were formed based on stacking of the lamellar-like assemblies, turned to fibrils with a twisted ribbon shape. The fibrils formed a network structure that was more homogeneous and denser than that the network formed by PalGH. Thus, molecular-level modulation of the assembly was amplified to induce the creation of the microscopic network structure. An important

fact is that a sol obtained by mechanically disrupting a mixed gel returns to a gel form spontaneously. Such behavior was not observed for the homo PalGH system. The sol-gel transition can be associated with the change in the fibril network but not with the molecular assembled state, which remains unchanged in the gel and the sol states. The difference in the mechanical response behaviors between the homo and the mixed gels may originate from the different morphology of their fibril network. The findings in this study should offer useful concepts in the development of supramolecular hydrogels that can undergo reversible sol-gel transition.

Acknowledgements

The synchrotron radiation facility experiments were performed at BL40B2 in the SPring8 with the approval of the Japan Synchrotron Radiation Research Institute (JASRI) (Proposal: 2014B1704). We thank Prof. Masahiro Goto and Dr. Rie Wakabayashi at Kyushu University for their help with confocal laser scanning microscopy. We thank Mr. Shun Fujita at Nissan Chemical Industries, Ltd. for his assistance during the TEM observation. This research was partly supported by a Grant-in-Aid for Scientific Research (A) (No. 15H02183) from the Ministry of Education, Culture, Sports, Science and Technology, Japan.

References

[a] *Department of Automotive Science, Kyushu University, Fukuoka 819-0395, Japan*
[b] *Nissan Chemical Industries, Ltd., Tokyo 101-0054, Japan. E-mail: matsumotoke@nissanchem.co.jp*
[c] *Department of Applied Chemistry, Kyushu University, Fukuoka 819-0395, Japan. E-mail: k-tanaka@cstf.kyushu-u.ac.jp, a-shundo@cstf.kyushu-u.ac.jp*
[d] *International Institute for Carbon-Neutral Energy Research (WPI-I2CNER), Kyushu University, Fukuoka 819-0395, Japan*

1. (*a*) S. Kiyokawa, K. Sugiyasu, S. Shinkai and I. Hamachi, *J. Am. Chem. Soc*., 2002, **124**, 10954; (*b*) K. Köhler, A. Meister, G. Föster, B. Dobner, S. Drescher, F. Ziethe, W. Richter, F. Steiniger, M. Drechsler, G. Hause and A. Blume, *Soft Matter*, 2006, **2**, 77; (*c*) G. Graf, S. Drescher, A. Meister, B. Dobner and A. Blume, *J. Phys. Chem. B*, 2011, **115**, 10478.
2. (*a*) S. R. Haines and R. G. Harrison, *Chem. Commun*., 2002, **23**, 2846; (*b*) H. Komatsu, S. Matsumoto, S. Tamaru, K. Kaneko, M. Ikeda and I. Hamachi, *J. Am. Chem. Soc*., 2009, **131**, 5580; (*c*) D. J. Adams, M. F. Bulter, W. J. Frith, M. Kirkland, L. Mullen and P. Sanderson, *Soft Matter*, 20009, **5**, 1856; (*d*) J. Raeburn, G. Pont, L. Chen, Y. Cesbron, R. Lévy and D. J. Adams, *Soft Matter*, 2012, **8**, 1168; (*e*) D. M. Wood, B. W. Greenland, A. L. Acton, F. R. Llansola, C. A. Murray, C. J. Cardin, J. F. Miravet, B. Escuder, I. W. Hamley and W. Hayes, *Chem. - Eur. J*., 2012, **18**, 2692.
3. (*a*) G. O. Llyoyd and J. W. Steed, *Nat. Chem.*, 2009, **1**, 437; (*b*) V. J. Nebot, J. J. O. Flores, J. Smerts, S. F. Prieto, B. Escuder and J. F. Miravet, *Chem. - Eur. J.*, 2014, **20**, 14465; (*c*) J. Li, I. Cvrtila, M. C. Delsuc. E. Otten and S. Otto, *Chem. - Eur. J.*, 2014, **20**, 15709.
4. (*a*) S. Matsumoto, S. Yamaguchi, S. Ueno, H. Komatsu, M. Ikeda, K. Ishizuka, Y. Ito, K. V. Tabata, H. Aoki, S. Ito, H. Noji and I. Hamachi, *Chem. - Eur. J.*, 2008, **14**, 3977; (*b*) Z. Qiu, H. Yu, J. Li, Y. Wang and Y. Zhang, *Chem. Commun.*, 2009, **23**, 3342; (*c*) X. Li, Y. Gao, Y. Kuang and B. Xu., *Chem. Commun.*, 2010, **46**, 5364.
5. (*a*) M. Shirakawa, N. Fujita and S. Shinaki, *J. Am. Chem. Soc.*, 2005, **127**, 4164; (*b*) X. Huang, S. R. Raghavan, P. Terech and R. G. Weiss, *J. Am. Chem. Soc*., 2006, **128**, 15341; (*c*) M. Xue, D. Gao, K. Liu, J. Peng and Y. Fang, *Tetrahedron*, 2009, **65**, 3369; (*d*) A. Shundo, K. Mizuguchi, M. Miyamoto, M. Goto and K. Tanaka, *Chem. Commun*., 2011, **47**, 8844; (*e*) A. Dawn, T. Shiraki, H. Ichikawa, A. Takada, Y. Takahashi, Y. Tsuchiya, L. T. N. Lien and S. Shinaki, *J. Am. Chem. Soc*., 2012, **134**, 2161; (*f*) X. Yu, X. Cao, L. Chen, H. Lan, B. Liu and T. Yi, *Soft Matter*, 2012, **8**, 3329; (*g*) D. Higashi, M. Yoshida and M. Yamanaka, *Chem. Asian J*. 2013, **8**, 2584.
6. (*a*) S. Ziane, S. Schlaubitz, S. Mirayx, A. Patwa, C. Lalande, I. Bilem, S. Lepreux, B. Rousseau, J. L. Meins, L. Latxague, P. Barthelemy and O. Chassande, *Eur. Cells Matter.*, 2012, **23**, 147; (*b*) A. Baral, S. Roy, A. Dehsorkhi, I. W. Hamley, S. Mohapatra, S. Ghosh and A. Banerjee, *Langmuir*, 2014, **30**, 929.
7. (*a*) Y. Gao, Y. Kuang, Z. Guo, Z. Guo, I. J. Krauss and B. Xu, *J. Am. Chem. Soc.*, 2009, **131**, 13576; (*b*) S. Soukasene, D. Toft, T. J. Moyer, H. Lu, H. K. Lee, S. M. Standley, V. L. Crynes and S. Stupp, *ACS Nano*, 2011, **5**, 9113; (*c*) J. Li, Y. Kuang, Y. Gao, X. Du, J. Shi and B. Xu, *J. Am. Chem. Soc.*, 2013, **135**, 542; (*d*) J. Liu, J. Liu, L. Chu, Y. Zhang, H. Xu, D. Kong, Z. Yang, C. Yang and D. Ding, *ACS Appl. Matter. Interfaces*, 2014, **6**, 5558.
8. (*a*) G. A. Silva, C. Czeisler, K. L. Niece, E. Beniash, D. A. Harrington, J. A. Kessler and S. I. Stupp, *Science*, 2004, **27**, 1352; (*b*) T. Liebmann, S. Rydholm, V. Akpe and H. Brismer, *BMC Biotechnology*, 2007, **7**, 88; (*c*) J. Li, R. Kooger, M. He, X. Xiao, L. Zheng and Y. Zhang, *Chem. Commun.*, 2014, **50**, 3722.
9. A. Shundo, Y. Hoshino, T. Higuchi, Y. Matsumoto, D. P. Penaloza Jr., K. Matsumoto, M. Ohno, K. Miyaji, M. Goto and K. Tanaka, *RSC Adv*., 2014, **4**, 36097.
10. (*a*) S. Roy, A. Baral, A. Banerjee, *Chem. - Eur. J.*, 2013, **19**, 14950; (*b*) S. Basak, J. Nanda and A. Banerjee, *Chem. Commun.*, 2014, **50**, 2356; (*c*) S. Saha, J. Bachi, T. Kundu, D. D. Diaz and R. Banerjee, *Chem. Commun.*, 2014, **50**, 3004.
11. (*a*) C. Yang, D. Li, Z. Liu, G. Hong, J. Zhang, D. Kong and Z. Yang, *J. Phys. Chem. B*, 2011, **116**, 633; (*b*) K. Munenobu, T. Hase, T. Oyoshi and M. Yamanaka, *Anal. Chem*., 2014, **86,** 9924.
12. (*a*) H. Hoshizawa, Y. Minemura, K. Yoshikawa, M. Suzuki and K. Hanabusa, *Langmuir*, 2013, **29**, 14466; (*b*) K. Liu and J. W. Steed, *Soft Matter*, 2013, **9**, 11699; (*c*) Y. Li, F. Zhou, Y. Wen, K. Liu, L. Chen, Y. Mao, S. Yang and T. Yi, *Soft Matter*, 2014, **10**, 3077.
13. (*a*) X. Y. Liu, P. D. Sawant, W. B. Tan, I. B. M. Noor, C. Pramesti and B. H. Chen, *J. Am. Chem. Soc.*, 2002, **124**, 15055; (*b*) D. M. Ryan, T. M. Doran and B. L. Nilsson, *Chem. Commun*., 2011, **47**, 475; (*c*) D. Li, J. Liu, L. Chu, J. Liu, Z. Yang, *Chem. Commun.*, 2012, **48**, 6175; (*d*) P. Bairi, P. Chakraborty, S. Mondal, B. Roy and A. K. Nandi, *Soft Matter*, 2014, **10**, 5114.
14. K. Matsumoto, A. Shundo, M. Ohno, S. Fujita, K. Saruhashi, N. Miyachi, K. Miyaji and K. Tanaka, *Phys. Chem. Chem. Phys.*, 2015, **17**, 2192.
15. Kakiuchi, N.; Shoji, T.; Hirasada, K.; Matsumoto, K.; Yama-guchi, H. Method for Preparing Lipopeptide Compound. US Patent, 0,253,012, October 4, 2012.
16. The strain amplitude dependence of storage modulus was examined at a frequency of 1.0 rad s^{-1}. The plateau modulus (G_P') in a lower strain amplitude region was simply proportional to the inverse of X. This makes it clear that there is no critical X value related to the gel formation itself.
17. (*a*) A. Meister, M. Bastrop, S. Koschoreck, V. M. Garamus, T. Sinemus, G. Hempel, S. Drescher, B. Dobner, W. Richterring, K. Huber and A. Blume, *Langmuir*, 2007, **23**, 7715; (*b*) Y. Nakagawa, H. Nakazawa and S. Kato, *J. Colloid Interface Sci.*, 2012, **376**, 146; (*c*) S. Song, R. Dong, Dong Wang, A. Song and J. Hao, *Soft Matter*, 2013, **9**, 4209.
18. (*a*) P. Terech, N. M. Sangeetha, B. Demé and U. Maitra, *J. Phys. Chem. B*, 2005, **109**, 12270; (*b*) S. Roy, A. Dasgupta and P. K. Das, *Langmuir*, 2007, **23**, 11769; (*c*) G. Cheng, V. Castelletto, R. R. Jones, C. J. Connon and I. W. Hamley, *Soft Matter*, 2011, **7**, 1326; (*d*) P. Duan, L. Qin, X. Zhu and M. Liu, *Chem. - Eur. J.*, 2011, **17**, 6389.
19. C. Tang, A. M. Smith, R. F. Collins, R. V. Ulijin and A. Saiani, *Langmuir*, 2009, **35**, 9447.
20. (*a*) J. H. Fuhrhop, P. Schnieder, E. Boekema and W. Helfrich, *J. Am. Chem. Soc.*, 1988, **110**, 2861; (*b*) A. Brizard, C. Aimé, T. Labrot, I. Huc, D. Berthier, F. Artzner, B. Desbat and R. Oda, *J. Am. Chem. Soc*., 2007, **129**, 3754; (*c*) E. T. Pashuck amd S. I. Stupp, *J. Am. Chem. Soc*., 2010,

132, 8819; (*d*) X. Zhu, P. Duan, L. Zhang and M. Liu, *Chem. - Eur. J.*, 2011, **17**, 3429.
21. It has been reported that the ribbon shape of a chiral molecular aggregate was controlled by its width. See: L. Ziserman, A. Mor. D. Harries and D. Danino, *Phys. Rev. Lett.*, 2011, **106**, 238105.
22. P. Greenspan, E. P. Mayer and S. D. Flower, *J. Cell. Biol.*, 1985, **100**, 965.
23. (*a*) M. C. A. Stuart, J. C. van de Pas and J. B. N. Engberts, *J. Phys. Org. Chem.*, 2005, **18**, 929; (*b*) C. B. Minkenberg, L. Florusse, R. Eelkema, G. J. M. Koper and J. H. van Esch, *J. Am. Chem. Soc.*, 2009, **131**, 11274; (*c*) J. H. Ryu, R. Roy, J. Ventura and S. Thayumanavan, *Langmuir*, 2010, **26**, 7086; (*d*) M. C. Morán, M. G. Miguel and B. Lindman, *Soft Matter*, 2011, **7**, 2001.
24. (*a*) X. Huang, S. R. Raghavan, P. Terech and R. G. Weiss, *J. Am. Chem. Soc.*, 2006, **128**, 15341; (*b*) P. Mukhopadhyay, N. Fujita, A. Tanada, T. Kishida, M. Shirakawa and S. Shinkai, *Angew. Chem. Int. Ed.*, 2010, **49**, 6338; (*c*) D. Penaloza, Jr., A. Shundo, K. Matsumoto, M. Ohno, K. Miyaji, M. Goto and K. Tanaka, *Soft Matter*, 2013, **9**, 5166.
25. (*a*) T. Shikata and H. Hirata, *Langmuir*, 1988, **4**, 354; (*b*) M. E. Cates and S. J. Candau, *J. Phys.: Condens. Matter,* 1990, **2**, 6869.